AAAS
Journal of Remote Sensing
Volume 2022, Article ID 9851013, 7 pages
https://doi.org/10.34133/2022/9851013

Journal of Remote Sensing
A SCIENCE PARTNER JOURNAL

Perspective

The Use of VGPM to Estimate Oceanic Primary Production: A "Tango" Difficult to Dance

Zhongping Lee[1,2] **and John F. Marra**[3]

[1]*State Key Lab of Marine Environmental Science, College of Earth and Ocean Sciences, Xiamen University, Xiamen, China*
[2]*School for the Environment, University of Massachusetts Boston, Boston, MA 02125, USA*
[3]*Brooklyn College of the City University of New York, Brooklyn, NY 11210, USA*

Correspondence should be addressed to Zhongping Lee; zhongping.lee@umb.edu

Received 12 April 2022; Accepted 6 June 2022; Published 29 June 2022

One of the primary goals of launching an ocean color satellite is to obtain over the global ocean synoptic measurements of primary production (PP), a measure of phytoplankton photosynthesis. To reach this ultimate goal, in addition to precise measurements of radiance at the satellite altitude and robust data processing systems, a key requirement is to link primary production with satellite-derived products, where a model must be developed and applied. Although many models have been developed in the past decades, the vertically generalized production model (VGPM) developed by Behrenfeld and Falkowski, due to its simplicity and ease of use with satellite products, has been a de facto "standard" for the estimation of PP from ocean color measurements over the past 20+ years. Thus, it has significantly influenced the ocean color remote sensing and the biological oceanographic communities. In this article, we discuss the limitations of VGPM (and PP models based on chlorophyll concentration) in estimating primary production.

1. Summary of VGPM

Phytoplankton are ubiquitous in aquatic ecosystems and play a critical role in the food web and in carbon and energy cycles. The growth of phytoplankton is driven by photosynthesis, and this process can be measured from carbon fixation or primary production (PP). Thus, it is no surprise that "rational estimate of the growth of phytoplankton over long periods and large regions … must be one of the central goals of biological oceanography" [1]. However, although there have been 10's of thousands in situ measurements of PP in the global ocean in the past 6+ decades since Steemann Neilsen introduced the ^{14}C tracer technique [2], it is "infinitesimal" in view of the tremendous size of the ocean where phytoplankton vary greatly in space and time. It has been concluded decades ago [1, 3, 4] that a combination of both in situ measurements and satellite remote sensing is the only feasible means to obtain a rational estimate of PP of the global ocean for different time windows.

Satellite sensors do not provide a direct measurement of PP, but rather related properties that can be used to estimate PP, where a model must be applied. This is basically a process to scale up discrete in situ data to broad-scale estimates guided or constrained by satellite measurements. Since such a model plays a key role in this process, many models have been developed over the past decades. In particular, because the concentration of chlorophyll-a (Chl, mg/m^3) is routinely measured in oceanic surveys and that chlorophyll-a is the critical pigment for photosynthesis, the mainstream models for PP estimation are centered on Chl. These include simple empirical models simply converting Chl to PP (e.g., [5, 6]), which was basically an extension after the invention of fast measurement of Chl in the field through measurement of chlorophyll-a fluorescence [7]. The performance of such simple models is not always robust; more importantly, these models are purely empirical, which cannot provide a cause-effect understanding for the estimation of PP.

To represent the process of phytoplankton photosynthesis or carbon fixation mechanistically, a general and conceptual function for PP at depth z and time t can be expressed as [4, 8, 9]

$$\mathrm{PP}(z,t,\lambda) = f\left(\mathrm{Chl}(z)\,;E(z,t,\lambda)\,;\alpha^B(z),P_m^B(z)\right). \quad (1)$$

Here, α^B is the initial slope of PP, while P_m^B is the asymptotic saturation rate at high light level, and both α^B and P_m^B are values normalized to chlorophyll concentration or biomass (B). To get water-column PP over time and include all the contributions for wavelengths in the 400-700 nm domain, it simply means an integration of Eq. (1) over time, depth, and wavelength (λ) [4]. Further, because conventionally Chl is taken as the key scaling parameter, and assuming that Chl of the global oceans can be well-estimated from satellite ocean color remote sensing, these models (after omitting wavelength dependence for brevity) can all be summarized in a conceptual form as [4, 10].

$$\mathrm{PP}(z,t) = \mathrm{Chl}(z) \times p\left(E(z,t)\,; \alpha^B(z), P_m^B(z)\right), \tag{2}$$

with function p for the chlorophyll-normalized (or biomass-normalized) primary production. For this function p, Sathyendranath and Platt [4] stated that "Many equations have been proposed to represent the function p, with varying degrees of analytical explanations to support them. However, from a practical point of view, it has been shown by Platt et al. (1977) that most of these equations yield similar results for water column integrals of primary production, which would suggest that the choice of equation for p(I) is not a crucial one …" Thus, it is not critical to spell out all the details of the various models regarding function p here. (The "I" in Sathyendranath and Platt [4] is the intensity of photosynthetically available radiation (PAR), which is represented as E in this article.)

To calculate PP(z, t, λ) mechanistically, as articulated in Sathyendranath and Platt [4], it is required to know the following: (1) the vertical profile of Chl, (2) the value of PAR at surface (E_0, units as mol quanta m^{-2}) and its propagation from surface to deeper depths (E (z)), and (3) the estimates of the photosynthesis-light parameters (i.e., α^B and P_m^B). Because ocean color remote sensing provides only averaged optical information of the upper layer of the water column, it is still a serious challenge even today to obtain accurate information of these properties over the water column, especially the photosynthesis-light parameters. Further, to obtain PP of large area over a long period of time, the complexity involved with Eqs. (1) and (2) poses a challenge for its broad application.

In view of the availability of both surface Chl and E_0 of the global ocean from satellite ocean color remote sensing, after analyzing more than 10,000 PP(z) profiles obtained from many regions of the global oceans, Behrenfeld and Falkowski [10] (represented as BF97 in the following) developed a simplified model for daily and water-column-integrated primary production. They bypassed the modeling of the details of p and focused instead on the P^B profiles of daily PP (note: symbols p and P^B represent the same property; since this article focuses on VGPM, we follow BF97 using P^B in the following for biomass-time-normalized PP), which is defined as

$$P^B(z) = \frac{\mathrm{PP}(z, \mathrm{daily})}{\mathrm{Chl}(z) \times D_{\mathrm{irr}}}. \tag{3}$$

Here, D_{irr} is the day length and measured in hours; thus, the units for P^B are mg C (mg Chl)$^{-1}$ h^{-1}. Figure 1 shows examples of vertical profiles of daily PP(z) and P^B (z). Subsequently, the focus of BF97 was on daily primary production, especially P^B, the "daily averaged" chlorophyll-normalized primary production, rather than the conceptual instantaneous property in Eq. (1).

For P^B (z), BF97 further found that its profiles follow a similar pattern and used a relative vertical distribution of P^B (here represented as P_{rel}^B instead of P_ζ^B in the original paper, as P_ζ^B and P^B (ζ) could be confused with each other), which is expressed as [10]

$$P_{\mathrm{rel}}^B(\zeta) = \left[1 - \exp\left(-\frac{E(\zeta)}{E_{\max}}\right)\right] \exp\left(-\beta_d \times E(\zeta)\right). \tag{4}$$

Here, ζ is an optical depth, which is the product of K and z, with K (in m^{-1}) for the attenuation coefficient of PAR and calculated from the euphotic zone depth (Z_{eu}, in meters)

$$K = \frac{-\ln(0.01)}{Z_{\mathrm{eu}}}, \tag{5}$$

and β_d is the photoinhibition parameter. Further, BF97 obtained daily water-column integrated primary production ($\mathrm{PP}_{\mathrm{eu\text{-}day}}$) as (note that the "–" sign in front of β_d in their original Eq. (8) was missing)

$$\begin{aligned}\mathrm{PP}_{\mathrm{eu-day}} = {} & \frac{P_{\mathrm{opt}}^B \times D_{\mathrm{irr}}}{\left[1 - \exp\left(-E_{\mathrm{opt}}/E_{\max}\right)\right] \exp\left(-\beta_d \times E_{\mathrm{opt}}\right)} \\ & \cdot \int_0^{Z_{\mathrm{eu}}} \left[1 - \exp\left(-\frac{E(z)}{E_{\max}}\right)\right] \exp\left(-\beta_d \times E(z)\right) \\ & \times \mathrm{Chl}(z) \times dz.\end{aligned} \tag{6}$$

Solar radiation (E (z)) at depth is (the expression in the original paper missed a "–" sign)

$$E(z) = E_0 \exp\left(-K \times z\right), \tag{7}$$

and E_{opt} is the solar radiation corresponding to the maximum P^B (represented as P_{opt}^B), which can be calculated from

$$E_{\mathrm{opt}} = E_0 \exp\left(-\zeta_{\mathrm{opt}}\right). \tag{8}$$

β_d and $E_{\max}$ are properties associated with photosynthesis [10]. Basically, Eq. (6) is the depth-resolved form of VGPM.

After empirically relating $E_{\max}$, ζ_{opt}, and β_d with E_0 [10], and considering Chl(z) can be moved out of the integration in Eq. (6) without much impact on $\mathrm{PP}_{\mathrm{eu\text{-}day}}$, BF97 finally

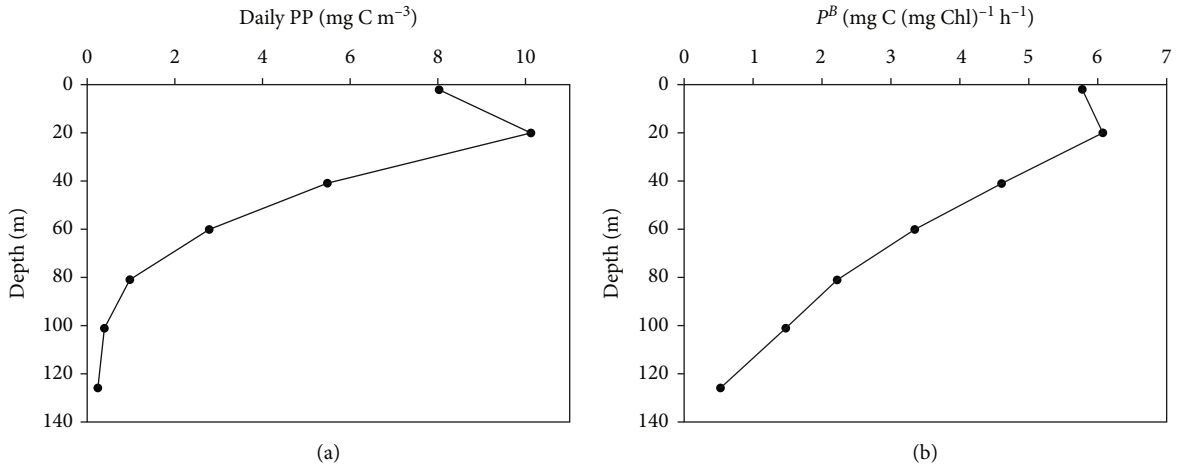

FIGURE 1: Examples (data from JFM) of daily PP profile (a) and the Chl-normalized, hourly, $P^B(z)$ profile (b). The reduction of PP near surface is due to photoinhibition of photosynthesis that is omitted in Eq. (1) for simplicity, but it can be easily incorporated.

obtained the widely used VGPM for daily depth-integrated primary production as (Eq. (10) of BF97)

$$\mathrm{PP}_{\mathrm{eu-day}} = 0.66125 \times P^B_{\mathrm{opt}} \times \frac{E_0}{E_0 + 4.1} \times Z_{\mathrm{eu}} \times \mathrm{Chl}_{\mathrm{opt}} \times D_{\mathrm{irr}}. \tag{9}$$

Note that the constant 4.1 has units as mol quanta m^{-2} for a day. The maximum biomass-normalized photosynthesis parameter (P^B_{opt}) was empirically parameterized from field data as a seventh-order polynomial function of temperature (T)

$$P^B_{\mathrm{opt}} = \sum_{i=0}^{7} v_i \times T^i. \tag{10}$$

Since E_0 and Chl (which can be approximated as $\mathrm{Chl}_{\mathrm{opt}}$ [10]) are standard products from ocean color satellites, T is available from satellites, Z_{eu} can be estimated from Chl [11], and D_{irr} can be easily calculated given date and location information, Eq. (9) becomes a very powerful and widely used tool to estimate daily water-column integrated PP of the global ocean.

This model for $\mathrm{PP}_{\mathrm{eu\text{-}day}}$ is more complex than empirical models simply based on Chl, such as that proposed a decade earlier by Eppley et al. [12], which is

$$\log\left(\mathrm{PP}_{\mathrm{eu-day}}\right) = 3 + 0.5 \log\left(\mathrm{Chl}\right), \tag{11}$$

where the Eppley model has no relationship of $\mathrm{PP}_{\mathrm{eu\text{-}day}}$ to solar radiation. Figure 2 presents ratios of $\mathrm{PP}_{\mathrm{eu\text{-}day}}$/Chl obtained from Eq. (9) for a range of Chl and common values of E_0 and T, which suggests that, for the same Chl, $\mathrm{PP}_{\mathrm{eu\text{-}day}}$ estimated from VGPM could be 2-3 times higher than that obtained by the Eppley model (its ratios of $\mathrm{PP}_{\mathrm{eu\text{-}day}}$/Chl for the same Chl are also included in Figure 2).

2. A Few Caveats

The processes to reach Eq. (9) are not straightforward, and some terms are not clearly described or represented by symbols and could cause confusion. For instance, P^B_{rel} (originally as P^B_{ζ}), a "dimensionless" quantity, is termed as "relative vertical distribution," but it was not clearly defined as "relative" to which property. Based on Figure 3(a) of BF97, it suggests that P^B_{rel} is defined as

$$P^B_{\mathrm{rel}}(z) = \frac{P^B(z)}{P^B\left(\zeta_{\mathrm{opt}}\right)}. \tag{12}$$

By this definition, P^B_{rel} is in a range of 0–1 for its vertical profile, matching the patterns showing in Figure 3(a) of BF97. However, this P^B_{rel} is not consistent with Eq. (4), as the maximum value calculated from Eq. (4) for normal β_d and E_{max} will be less than 1. This difference suggests that although Eq. (4) represents a "relative vertical distribution," it is not necessarily that of Eq. (12). As such, in order to compensate for the maximum value of Eq. (4) is less than 1, the following term

$$\left[1 - \exp\left(-\frac{E_{\mathrm{opt}}}{E_{\mathrm{max}}}\right)\right] \exp\left(-\beta_d \times E_{\mathrm{opt}}\right) \tag{13}$$

is included in Eq. (6) as a denominator. Note that if P^B_{rel} is defined following Eq. (12) and modeled matching that showing in Figure 3(a) of BF97, there is no need to have such a denominator in Eq. (6).

Further, in the process to reach the final form for $\mathrm{PP}_{\mathrm{eu}}$ (Eq. (9)), BF97 obtained the following integration (which is Eq. (9) of BF97)

$$\int_z P^B_{\mathrm{rel}}(\zeta) = \frac{E_0}{E_0 + 4.1}. \tag{14}$$

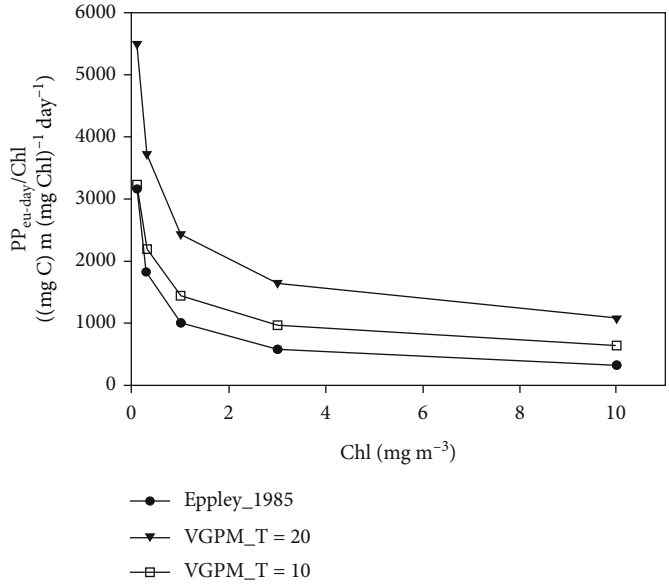

FIGURE 2: A comparison of $PP_{eu\text{-}day}$/Chl for Chl in a range of 0.1–10 mg m^{-3} calculated from VGPM and from the Eppley model. The temperatures used are included in the figure, while E_0 is kept as 40 mol quanta m^{-2} and D_{irr} as 12 hours.

For a function as Eq. (4), there is no analytical solution for its integration over depth. Further, no matter if P^B_{rel} are the profiles shown in Figure 3(a) of BF97 or those represented by Eq. (4), the integration over depth in the left side of Eq. (14) will be greater than 1.0, while the right side of Eq. (14) will be always less than 1.0. This mismatch suggests that there must be a scaling somewhere in the integration in order to reach Eq. (14).

Since Eq. (14) could not be derived analytically, Eq. (9) was obtained through numerical simulations (Dr. Michael Behrenfeld, personal communication) and consequently, Eq. (9) is not exactly equal to Eq. (6). For E_0 in a range of 5–50 mol quanta m^{-2} and Z_{eu} in a range of 20–200 m, the ratio of Eq. (9) to Eq. (6) is in a range of 0.75-1.07, with higher deviation from 1 at low E_0. Compared to the large uncertainties in field measurement of primary production, this deviation in the numerical reduction of Eq. (6) to Eq. (9) is insignificant. This also indicates that the constant "0.66125" in Eq. (9) can be rounded to "0.7" or "0.66" without any significant impact on the performance of VGPM.

3. The "Tangling" of VGPM or Chl-Based PP Model

Tango, involving exciting movements, is a popular dance that originated in Argentina and is a pleasure to watch. VGPM, due to its simplicity and reasonable performance shown in BF97, is also very exciting for the biological oceanographic community. Tango requires two partners to cooperate nicely and precisely. For VGPM, since E_0 and D_{irr} can be well estimated, and Z_{eu} can be estimated from Chl, it also requires two key "partners" to cooperate nicely. The two are Chl and P^B_{opt}, but the "tango," a tangling of optics, biology and physiological properties in remote sensing models, makes the "dance" not the level of a great show yet. Here are the reasons.

(1) Presently, the Chl product of the global ocean from satellite ocean color measurements is generated with empirical algorithms, either band ratio [13] or band difference [14] (collectively termed as color index, CI) of the remote sensing reflectance (R_{rs}). This CI, at least for oceanic waters, as illustrated in the literature [14, 15], represents the total absorption coefficient (a) at the blue wavelength (normally around 443 nm), where a (443) can be expressed as

$$a(443) = a_w(443) + a^*_{ph}(443) \times Chl + a_{dg}(443). \quad (15)$$

Here, $a_w(443)$ is the absorption coefficient of pure (sea)water [16, 17], which varies slightly with temperature [18, 19], $a^*_{ph}(443)$ is the chlorophyll-specific absorption coefficient, and a_{dg} is the absorption coefficient of detritus-gelbstoff. Thus, in addition to Chl, there are two "extra" variables governing the variation of $a(443)$: $a^*_{ph}(443)$ and $a_{dg}(443)$. Even considering $a_{dg}(443)$ to covary with Chl, the variation of $a^*_{ph}(443)$ needs to be taken into account before we can accurately estimate Chl based on CI. An unpleasant truth is that $a^*_{ph}(443)$ of the global ocean varies widely for the same Chl value [20], and there is still a big knowledge gap on an appropriate estimation of $a^*_{ph}(443)$ from remote sensing. Without an understanding of the spatial-temporal variation of $a^*_{ph}(443)$, in the estimation of Chl from ocean color measurements we will be stalled at the current level [21].

(2) P^B_{opt}, the "maximum C fixation rate within a water column", is far from a constant (with its variation more than a factor of 2) for the same temperature (see Figure 7 in BF97) and varies in a complex manner. Following the same principle but taking a different mathematical form from Eq. (1), instantaneous PP can be expressed as [22–24]

$$\mathrm{PP}(z,t,\lambda) = 12\mathrm{Chl}(z,t) \times a^*_{ph}(z,t,\lambda) \times E(z,t,\lambda) \times \phi(z,t,\lambda). \quad (16)$$

Here, ϕ is the photosynthetic quantum yield, and the constant 12 converts mol carbon to gram carbon. Thus, after integration over time and wavelength, Eq. (16) indicates that P^B_{opt} is

$$P^B_{\mathrm{opt}} = \frac{PP(z)}{\mathrm{Chl}(z) \times D_{\mathrm{irr}}}\bigg|_{\max} \propto a^*_{ph}(z) \times E(z) \times \phi(z)\bigg|_{\max}. \quad (17)$$

This expression suggests that the value of P^B_{opt} depends on three properties: solar radiation (E), photophysiology (ϕ), and a^*_{ph} at the depth (opt) where P^B is the maximum. This multivariate dependence of P^B_{opt} may explain why there are large variations of P^B_{opt} obtained from in situ measurements [10]. Consequently, it is difficult, if not impossible, to accurately estimate P^B_{opt} using temperature alone (Eq. (10)). As highlighted in Behrenfeld and Falkowski [10], "the accuracy of productivity algorithms in estimating $\mathrm{PP}_{\mathrm{eu}}$ is dependent primarily upon the ability to accurately represent variability in P^B_{opt}." However, since a^*_{ph}, a bio-optical property that varies widely, is a variable of P^B_{opt} (see Eq. (17)), an accurate estimation of P^B_{opt} remains challenging. This might be the main reason that Behrenfeld et al. [25] later concluded "… a clear path for globally modeling or remotely observing variability in chlorophyll-specific photosynthesis has even to this day never been identified."

4. Schemes to "Detangling" Optics and Biology for PP Estimation

From the above discussions, the biggest uncertainties in the remote sensing of PP via VGPM or similar Chl-based models is the "tangling" of optical and biological properties that is hooked explicitly or implicitly by a^*_{ph}; thus, a detangling, i.e., a tango to allowing space for the two partners, is certainly plausible. Detangling can be achieved by excluding the involvement of a^*_{ph}. There have been two schemes proposed in the past decades for this. One is centered on the absorption coefficient of phytoplankton (a_{ph}) [26] or the absorption-based approach (AbPM). Another, the "carbon-based approach" (CbPM) [25, 27] is centered on the backscattering coefficients of phytoplankton.

The AbPM scheme is a rearrangement of Eq. (16):

$$\mathrm{PP}(z,t,\lambda) = 12\, a_{\mathrm{ph}}(z,t,\lambda) \times E(z,t,\lambda) \times \phi(z,t,\lambda), \quad (18)$$

as by definition a_{ph} is the product of Chl and a^*_{ph}. In this equation, a_{ph} is an optical property while ϕ is a biological (or photophysiological) property. They are two different and independent properties that are not tangled or hooked by a^*_{ph}. While the value and variation of ϕ have to be determined from in situ measurements, a_{ph} can be directly and analytically inverted from R_{rs} [28]. It is a_{ph} and ϕ (E is a minor player as ϕ also varies with E) working together, a "tango", to complete the estimation of PP from ocean color remote sensing, where significantly better estimates have been demonstrated [26, 29–31]. This might be the "tango" we should practice for the remote sensing of oceanic PP.

The CbPM scheme focuses on the phytoplankton biomass (C_{ph}) with C_{ph} estimated from remotely sensed particle backscattering coefficient (b_{bp}). Although an empirical relationship is required to convert b_{bp} to C_{ph}, where nonnegligible uncertainties exist, it also avoided the involvement of a^*_{ph} and showed promising results in explaining the decadal variations of global PP [25].

Nevertheless, by no means do we suggest that the above schemes have resolved all the issues and challenges associated with the remote sensing of PP, especially the vertical variations associated with biological and physiological properties [32–34]. Rather, it only indicates that it is not a requirement to include Chl (and then the involvement of a^*_{ph}) in the algorithms or models. If Chl is included, the optical and biological properties will be tangled for the estimation of oceanic PP from ocean color remote sensing.

5. Concluding Remarks

Although remote sensing of global PP based on ocean color measurements has been carried out for more than four decades, we are still far from the goal of achieving an accurate estimation of the spatial and temporal distributions of PP of the global oceans. While the VGPM developed by Behrenfeld and Falkowski [10] significantly advanced the application of satellite data for PP estimation and contributed to the overall estimates of global annual PP, the implicit embedding of a^*_{ph} in the determination of both Chl and P^B_{opt}, the two key players of VGPM and many other Chl-based models, makes the estimated PP for a region and at a specific time to have large uncertainties. To achieve more reliable PP estimates at regional and temporal scales, and to improve further the remote sensing of optical properties (especially a_{ph} and the backscattering coefficient of phytoplankton) from ocean color data and to obtain its vertical information, it is critical to have a better understanding and handling of the quantum yield of phytoplankton photosynthesis, where knowledge of phytoplankton functional types is important.

Conflicts of Interest

The authors declare that they have no known conflict of interest or personal relationships that could have appeared to influence the work reported in this paper.

Acknowledgments

Dr. Michael Behrenfeld provided comments and suggestions on an earlier version of this manuscript, which are greatly appreciated. We thank two anonymous reviewers for constructive comments and suggestions and the National Natural Science Foundation of China (#41830102, #41941008, #41890803) for support of this work.

References

[1] A. Longhurst, S. Sathyendranath, T. Platt, and C. Caverhill, "An estimate of global primary production in the ocean from satellite radiometer data," *Journal of Plankton Research*, vol. 17, no. 6, pp. 1245–1271, 1995.

[2] E. Steemann Neilsen, "The use of radio-active carbon (C14) for measuring organic production in the sea," *Journal du Conseil / Conseil Permanent International pour l'Exploration de la Mer*, vol. 18, pp. 117–140, 1952.

[3] M. J. Perry, "Assessing marine primary production from space," *Bioscience*, vol. 36, no. 7, pp. 461–467, 1986.

[4] S. Sathyendranath and T. Platt, "Underwater light field and primary production: application to remote sensing," in *Ocean Colour: Theory and Applications in a Decade of CZCS Experience*, V. Barale and P. M. Schlittenhardt, Eds., pp. 79–93, ECSC, EEC, EAEC: Brussels and Luxembourg, 1993.

[5] R. Margalef, "Primary productivity and structure of communities," *Mem. Ist. Ital. Idrobiol*, pp. 1–14, 1965.

[6] R. C. Smith, R. W. Eppley, and K. S. Baker, "Correlation of primary production as measured aboard ship in southern-California coastal waters and as estimated from satellite chlorophyll images," *Marine Biology*, vol. 66, no. 3, pp. 281–288, 1982.

[7] C. S. Yentsch and D. W. Menzel, "A method for the determination of phytoplankton chlorophyll and phaeophytin by fluorescence," *Deep-Sea Research*, vol. 10, no. 3, pp. 221–231, 1963.

[8] T. Platt, "Remote sensing of phytoplankton in the sea: surface-layer chlorophyll as an estimate of water-column chlorophyll and primary production," *International Journal of Remote Sensing*, vol. 4, no. 2, pp. 343–351, 1983.

[9] T. Platt, "Primary production of the ocean water column as a function of surface light intensity: algorithms for remote sensing," *Deep Sea Research*, vol. 33, no. 2, pp. 149–163, 1986.

[10] M. J. Behrenfeld and P. G. Falkowski, "Photosynthetic rates derived from satellite-based chlorophyll concentration," *Limnology and Oceanography*, vol. 42, no. 1, pp. 1–20, 1997.

[11] A. Morel, "Optical modeling of the upper ocean in relation to its biogenous matter content (case I waters)," *Journal of Geophysical Research*, vol. 93, no. C9, pp. 10749–10768, 1988.

[12] R. Eppley, E. Steward, M. Abbott, and U. Heyman, "Estimating ocean primary production from satellite chlorophyll: introduction to regional differences and statistics for the southern California bight," *Journal of Plankton Research*, vol. 7, no. 1, pp. 57–70, 1985.

[13] J. O'Reilly, S. Maritorena, B. G. Mitchell et al., "Ocean color chlorophyll algorithms for SeaWiFS," *Journal of Geophysical Research*, vol. 103, no. C11, pp. 24937–24953, 1998.

[14] C. Hu, Z. Lee, and B. Franz, "Chlorophyllaalgorithms for oligotrophic oceans: a novel approach based on three-band reflectance difference," *Journal of Geophysical Research*, vol. 117, no. C1, p. C01011, 2012.

[15] H. R. Gordon and A. Morel, *Remote assessment of ocean color for interpretation of satellite visible imagery: A review*, Springer-Verlag, New York, 1983.

[16] Z. Lee, J. Wei, K. Voss, M. Lewis, A. Bricaud, and Y. Huot, "Hyperspectral absorption coefficient of "Pure" seawater in the range of 350–550 nm inverted from remote sensing reflectance," *Applied Optics*, vol. 54, no. 3, pp. 546–558, 2015.

[17] J. D. Mason, M. T. Cone, and E. S. Fry, "Ultraviolet (250–550 nm) absorption spectrum of pure water," *Applied Optics*, vol. 55, no. 25, pp. 7163–7172, 2016.

[18] R. Rottgers, D. McKee, and C. Utschig, "Temperature and salinity correction coefficients for light absorption by water in the visible to infrared spectral region," *Optics Express*, vol. 22, no. 21, pp. 25093–25108, 2014.

[19] G. Wei, Z. Lee, X. Wu, X. Yu, S. Shang, and R. Letelier, "Impact of temperature on absorption coefficient of pure seawater in the blue wavelengths inferred from satellite andin situmeasurements," *Journal of Remote Sensing*, vol. 2021, article 9842702, 13 pages, 2021.

[20] A. Bricaud, M. Babin, A. Morel, and H. Claustre, "Variability in the chlorophyll-specific absorption coefficients of natural phytoplankton: analysis and parameterization," *Journal of Geophysical Research*, vol. 100, no. C7, pp. 13321–13332, 1995.

[21] Z. Lee, S. Shang, S. Zhang, J. Wu, G. Wei, and X. Wu, "Impact of temporal variation of chlorophyll-specific absorption on phytoplankton phenology observed from ocean color satellite: a numerical experiment," *Oceans*, vol. 125, no. 12, p. e2020JC016382, 2020.

[22] D. Antoine and A. Morel, "Oceanic primary production: 1. Adaptation of a spectral light-photosynthesis model in view of application to satellite chlorophyll observations," *Global Biogeochemical Cycles*, vol. 10, no. 1, pp. 43–55, 1996.

[23] M. J. Behrenfeld and P. G. Falkowski, "A consumer's guide to phytoplankton primary productivity models," *Limnology and Oceanography*, vol. 42, no. 7, pp. 1479–1491, 1997.

[24] A. Morel, "Light and marine photosynthesis: a spectral model with geochemical and climatological implications," *Progress in Oceanography*, vol. 26, no. 3, pp. 263–306, 1991.

[25] M. J. Behrenfeld, E. Boss, D. Siegel, and D. M. Shea, "Carbon-Based Ocean productivity and phytoplankton physiology from space," *Global Biogeochemical Cycles*, vol. 19, no. 1, 2005.

[26] Z. P. Lee, K. L. Carder, J. Marra, R. G. Steward, and M. J. Perry, "Estimating primary production at depth from remote sensing," *Applied Optics*, vol. 35, no. 3, pp. 463–474, 1996.

[27] T. Westberry, M. J. Behrenfeld, D. A. Siegel, and E. Boss, "Carbon-based primary productivity modeling with vertically resolved photoacclimation," *Global Biogeochemical Cycles*, vol. 22, no. 2, 2008.

[28] Z. P. Lee and K. L. Carder, "Absorption spectrum of phytoplankton pigments derived from hyperspectral remote-sensing reflectance," *Remote Sensing of Environment*, vol. 89, no. 3, pp. 361–368, 2004.

[29] J. Marra, C. C. Trees, and J. E. O'Reilly, "Phytoplankton pigment absorption: a strong predictor of primary productivity in the surface ocean," *Deep Sea Research*, vol. 54, no. 2, pp. 155–163, 2007.

[30] Z. Lee, V. P. Lance, S. Shang et al., "An assessment of optical properties and primary production derived from remote sensing in the Southern Ocean (SO GasEx)," *Journal of Geophysical Research*, vol. 116, 2011.

[31] G. M. Silsbe, M. J. Behrenfeld, K. H. Halsey, A. J. Milligan, and T. K. Westberry, "The CAFE model: a net production model for global ocean phytoplankton," *Global Biogeochemical Cycles*, vol. 30, no. 12, pp. 1756–1777, 2016.

[32] Y.-Y. Shih, F.-K. Shiah, C.-C. Lai et al., "Comparison of primary production using in situ and satellite-derived values at the SEATS Station in the South China Sea," *Frontiers in Marine Science*, vol. 8, p. 747763, 2021.

[33] S. Sathyendranath and T. Platt, "The spectral irradiance field at the surface and in the interior of the ocean: a model for applications in oceanography and remote sensing," *Journal of Geophysical Research*, vol. 93, no. C8, pp. 9270–9280, 1988.

[34] J. S. Long, A. J. Fassbender, and M. L. Estapa, "Depth-resolved net primary production in the Northeast Pacific Ocean: a comparison of satellite and profiling float estimates in the context of two marine heatwaves," *Geophysical Research Letters*, vol. 48, no. 19, p. e2021GL093462, 2021.